Cluster Monte Carlo simulations of phase transitions and critical phenomena in zeolites

Ilija Dukovski and Jonathan Machta
Department of Physics and Astronomy, University of Massachusetts, Amherst, Massachusetts 01003

Chandra Saravanan[a)]
Department of Chemistry, University of Massachusetts, Amherst, Massachusetts 01003

Scott M. Auerbach[b)]
Department of Chemistry, Department of Chemical Engineering, University of Massachusetts, Amherst, Massachusetts 01003

(Received 16 March 2000; accepted 5 June 2000)

We simulated benzene adsorption in Na–X and Na–Y zeolites on a lattice of binding sites using a two-replica cluster Monte Carlo algorithm. Evidence for a vapor–liquid phase transition is explored for a range of guest–guest and host–guest energy and entropy parameters. The critical temperature is found to vanish precipitously with increasing energy difference between sites. For Na–X, critical temperatures as high as 300–400 K are found for reasonable values of the parameters, while for Na–Y no phase transition is predicted. © *2000 American Institute of Physics*. [S0021-9606(00)70433-8]

I. INTRODUCTION

The thermodynamic properties of confined fluids play a central role in separation and reactions that take place within porous materials.[1,2] Of particular interest are hysteresis loops and precipitous jumps in adsorption isotherms, since these are often associated with vapor–liquid transitions of the confined fluid. Although there is a vast literature on such transitions in mesoporous materials, there are very few reports of phase transitions in microporous solids such as zeolites. This is presumably because confinement into such small cavities (<20 Å) can reduce the vapor–liquid critical temperature to extremely low values or even eliminate coexistence altogether. Nevertheless, there have been occasional reports of possible phase transitions in such systems. For example, hysteresis loops have been observed at 77 K for methane in $AlPO_4$–5, a one-dimensional channel zeolite. Radhakrishnan and Gubbins[3] simulated this system taking into account interactions between methanes in adjacent pores and found a critical temperature of 52 K. However, the simulations of Maris *et al.*[4] suggest that the interactions between methane molecules in adjacent channels do not account for the observed transition. For benzene in Na–Y, a multiple-quantum proton nuclear magnetic resonance (NMR) study detected a continuous network of coupled proton spins,[5] suggesting the importance of interactions among molecules in adjacent cages. These experimental and theoretical studies suggest that first-order phase transitions and critical phenomena may be possible for molecules in microporous solids.

In a previous study, Saravanan and Auerbach[6] used grand canonical Monte Carlo[7] (GCMC) and thermodynamic integration[8–10] (TI) to demonstrate that cooperative cage-to-cage interactions can lead to vapor–liquid transitions for benzene in Na–X zeolite. In Ref. 6 the system was modeled by a lattice gas on a decorated diamond lattice with two types of binding sites (see Fig. 1). Although this lattice model provides a good approximation to the actual adsorption site topology, its accuracy is limited by the uncertainties of the input parameters in the Monte Carlo (MC) simulations. Some of the parameters were obtained from experimental thermochemistry[11,12] but others are more difficult to estimate. Uncertainties in these parameters yield uncertainty in the critical temperature, and possibly even uncertainty regarding the existence of the phase transition. Since Saravanan and Auerbach only considered a single set of parameter values, the uncertainty in the critical temperature is completely unknown. In the present paper, we apply a novel cluster algorithm to efficiently simulate benzene in Na–X and Na–Y for a wide range of parameters using the lattice gas model in Ref. 6. One of our primary results is that the phase transition can be completely suppressed by modestly increasing the energy difference between different benzene binding sites.

The thermodynamic integration (TI) technique used in Ref. 6 exploits the fact that the chemical potentials and grand potential densities (essentially pressures) must be equal for the coexisting phases in equilibrium. Saravanan and Auerbach applied TI to determine the grand potential density as a function of chemical potential for the vapor and liquid phases separately. This was accomplished using a Metropolis algorithm that updates one site at a time, and therefore, remains in one phase for long times due to the free energy barrier between the two phases. Unfortunately, TI breaks down as the critical region is approached from the low-temperature side, for one of two reasons. For small systems, the free energy barrier between phases becomes small and

[a)]Present address: Department of Chemistry, UC Berkeley, Berkeley, CA 94720
[b)]Author to whom correspondence should be addressed. Electronic mail: auerbach@chem.umass.edu

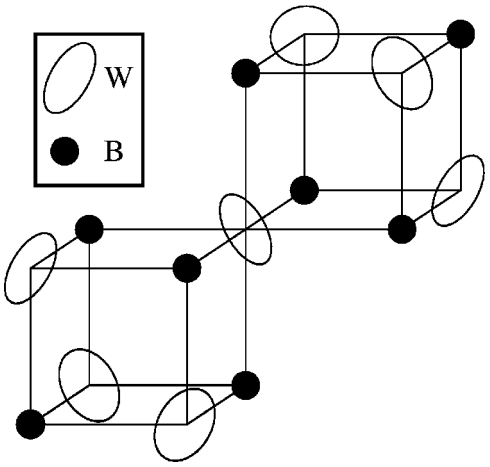

FIG. 1. Lattice structure of benzene adsorption sites in Na–X and Na–Y: B-sites are near Na cations, while W-sites are in windows separating adjacent cages.

the distinction between the two phases diminishes, making it difficult to separately determine the grand potential density for each phase. Since the free energy barrier between phases grows with system size, one might try to avoid this difficulty by simulating larger systems. However, for large systems, the Metropolis algorithm has very long equilibration times near the critical point, a phenomenon known as critical slowing. For these reasons, Saravanan and Auerbach were not able to closely approach the critical point. Instead, they were forced to extrapolate the location of the critical point using data from the subcritical region by assuming that the coexistence curve obeys the three-dimensional Ising scaling law.

In the present paper we apply a novel Monte Carlo algorithm that partially avoids the difficulties inherent in the TI method. We implement a two-replica cluster algorithm,[13–15] which updates (flips) large clusters of spins in a single step. Unlike local algorithms such as the Metropolis algorithm, which remain in a single phase for a long time, the two-replica algorithm can jump between phases in a single Monte Carlo step. In addition, the two-replica algorithm suffers less critical slowing than the Metropolis algorithm. Thus we are able to simulate relatively large systems in both the subcritical and critical regions.

Our results show that for Na–X, critical temperatures as high as 300–400 K can be found for reasonable values of the parameters, while for Na–Y no phase transition is found. The critical temperature is suppressed to zero for sufficiently large differences between the binding energies. Below, in Sec. IV, we explain how this suppression of T_c can be understood in the context of a simpler spin model, the Ising model in a staggered field. The strong sensitivity of the critical temperature on system parameters highlights the need for more precise experimental characterization of benzene in Na–X and related systems.

The remainder of this paper is organized as follows: In Sec. II we describe the model of benzene in Na–X and Na–Y zeolites. Section III provides a brief description of the two-replica algorithm implemented in this study. In Sec. IV we present the results of our study and compare them with the results in Ref. 6, and in Sec. V we conclude.

II. GENERAL MODEL

We model benzene adsorption in Na–X and Na–Y by replacing the zeolite framework with a three-dimensional lattice of binding sites. Benzene has two predominant sites in Na–Y,[16] shown schematically in Fig. 1. In the black (B) site in Fig. 1, benzene enjoys favorable charge–quadrupole interactions with a nearby Na cation. In the white (W) site in Fig. 1, which is less stable than the black site, benzene lies in the plane of the window separating adjacent supercages.

Locating benzene adsorption sites in Na–X is more difficult because of the influence of additional Na cations in low-symmetry positions near the windows. Recent crystallographic studies[17,18] favor the prevalence of Na cations that lie in the window, which would preclude benzene from lying in the plane of the Na–X window, as it does in Na–Y. Indeed, the powder neutron diffraction study of Vitale *et al.*[17] found benzene in Na–X only at the black sites, but located only half the adsorbed benzene, suggesting that low-symmetry benzene sites near the windows are likely. These binding sites would act as intermediates for cage-to-cage interactions, in analogy with Na–Y W sites. As such, we denote benzene sites near window cations as Na–X W sites, although their geometries and energies differ from those of Na–Y W sites. The lattice of benzene binding sites in Na–X and Na–Y thus contains four tetrahedrally arranged B sites and four tetrahedrally arranged, doubly shared W sites per supercage. Saturation coverages of $\sim$6 molecules per cage are found for benzene in Na–X and Na–Y,[11] corresponding to occupation of all B and W sites. In equations that follow, the W and B sites are denoted sites 1 and 2, respectively.

A lattice gas model is used to describe the thermodynamics of these systems, limiting the range of adsorbate–adsorbate interactions to nearest neighbors. The Hamiltonian for a lattice with M_1 W sites and $M_2=2M_1$ B sites, takes the form:

$$H(\mathbf{n},\mathbf{m})=\sum_{i=1}^{M_1} n_i f_1+\frac{1}{2}\sum_{i,j=1}^{M_1} n_i J_{ij}^{11} n_j+\sum_{i=1}^{M_1}\sum_{j=1}^{M_2} n_i J_{ij}^{12} m_j + \frac{1}{2}\sum_{i,j=1}^{M_2} m_i J_{ij}^{22} m_j+\sum_{i=1}^{M_2} m_i f_2, \tag{1}$$

where $\mathbf{n}$ and $\mathbf{m}$ are site occupation numbers for W and B sites, respectively. f_1 and f_2 are site free energies given by $f_i=\varepsilon_i-\mu-Ts_i$, where μ is the chemical potential. In Eq. (1), J_{ij}^{11}, J_{ij}^{12}, and J_{ij}^{22} are the nearest-neighbor W–W, W–B, and B–B interactions, respectively, i.e., $J_{ij}^{11}=J_{11}$ for nearest-neighbor W sites and zero otherwise, and so on for J_{ij}^{12} and J_{ij}^{22}. In previous studies we have used the following site binding energies: $\varepsilon_2=-0.78$ eV and $\varepsilon_1=-0.63$ eV for benzene in Na–X,[19] and $\varepsilon_2=-0.78$ eV and $\varepsilon_1=-0.53$ eV for benzene in Na–Y.[6]

Site 2 is chosen for the zero of entropy in both Na–X and Na–Y, giving $s_2 \equiv 0$. Monte Carlo simulations for benzene in Na–Y have shown that site 1 is favored entropically, with a temperature-independent equilibrium coefficient prefactor of $\sim$7.2,[20] which more than compensates for the fact that there are twice as many B sites as W sites. This makes

$s_1 = k_B \ln(7.2) = 1.98 k_B$ for benzene in Na–Y, which we have assumed in previous studies also holds for benzene in Na–X.[6]

The adsorbate–adsorbate parameters, J_{ij}, are obtained from the second virial coefficient of the heat of adsorption,[11,12] yielding $J = J_{12} = J_{22} \cong -0.04$ eV. J_{11} is set to zero because the W–W intracage distance is larger than typical B–B and W–B intracage distances, i.e., $d(\mathrm{B,B}) \approx d(\mathrm{B,W}) \approx 5$ Å, while $d(\mathrm{W,W}) \approx 9$ Å.[16]

The results we find below are particularly sensitive to the parameter $(f_1 - f_2)/|J|$, of which f_1 is the most poorly known. To determine the sensitivity of the critical temperature to changes in f_1, we varied both ε_1 and s_1 over physically relevant ranges. The physically relevant range for ε_1 is determined by considering initial enthalpies of benzene adsorption in weakly adsorbing and strongly adsorbing zeolites with the same topology as Na–X and Na–Y. These range from -0.78 eV for strong adsorption[11,12] to -0.55 eV for weak adsorption.[21] Below we study the range $\varepsilon_1 \in [-0.78, -0.60]$ eV, because the phase transition is already completely suppressed for $\varepsilon_1 = -0.60$ eV. The physically relevant range for s_1 is determined by considering vibrational freedom at W sites. As discussed above, we have performed Monte Carlo simulations yielding $s_1 = 1.98 k_B$ for benzene in Na–Y,[20] showing that benzene in Na–Y has more vibrational freedom in W sites than it does in B sites. Because the Na–X W site is presumed to involve coordination to Na, which tends to restrict vibrational motion, it is likely that $0 \leqslant s_1 \leqslant 1.98 k_B$ for benzene in Na–X. Finally, to determine qualitatively how adsorbate–adsorbate interactions control the nature and existence of this phase transition, we varied J_{22} over the range 0 to -0.05 eV.

In order to conveniently apply cluster Monte Carlo methods to lattice gas models, we map the lattice gas model onto the corresponding Ising spin model. This mapping is also convenient for interpreting our results below, because the effects of varying parameters in the Ising model are simpler to understand than those from varying lattice gas parameters. The Ising model involves interacting magnetic spins that take values of ± 1. The mapping of the lattice gas model into the Ising model is given with the equations:

$$\tau_i = 2n_i - 1, \tag{2}$$

$$\sigma_i = 2m_i - 1, \tag{3}$$

where n_i and m_i are the occupation numbers (taking values 0 and 1) of the lattice gas model, while τ_i and σ_i are the spin variables (taking values -1 and 1) of the Ising model, for W and B sites, respectively. The binding energies of the lattice gas model map into internal magnetic fields in the Ising model, while the chemical potential maps into an external magnetic field. The Hamiltonian of the system after the mapping into the Ising model is

$$H(\boldsymbol{\tau}, \boldsymbol{\sigma}) = \sum_{i=1}^{M_1} \tau_i h_1 + \frac{1}{2} \sum_{i,j=1}^{M_1} \tau_i K_{ij}^{11} \tau_j + \sum_{i=1}^{M_1} \sum_{j=1}^{M_2} \tau_i K_{ij}^{12} \sigma_j + \frac{1}{2} \sum_{i,j=1}^{M_2} \sigma_i K_{ij}^{22} \sigma_j + \sum_{i=1}^{M_2} \sigma_i h_2, \tag{4}$$

where $K_{ij}^{11} = K_{11} = J_{11}/4$ for nearest-neighbor W–W interactions, and zero otherwise. Likewise $K_{12} = J_{12}/4$ and $K_{22} = J_{22}/4$ for the other nearest-neighbor interactions. In addition, the internal magnetic fields are given by $h_1 = f_1/2 + 6K_{12}$ and $h_2 = f_2/2 + 6K_{22}$ for W and B sites, respectively.

III. SIMULATION METHODS

In this study we use a cluster Monte Carlo technique[22–24] to simulate the Ising model of Eq. (4). Our approach is similar to the single cluster method introduced by Wolff, which we now briefly describe. First a ''seed'' site for the cluster is randomly chosen. Next, neighbors of the seed site with the same spin as the seed site are added to the cluster with probability $p = 1 - e^{-2K/k_B T}$ where K is the Ising coupling strength for the bond connecting the seed to the neighbor. Spins with the opposite value as the seed spin are not added to the cluster. The growth process continues by adding spins on the perimeter of the cluster with probability p. After no more sites can be added to the cluster, the cluster is flipped, that is, every spin in the cluster is reversed. It is straightforward to prove detailed balance, ergodicity and, thus, convergence to equilibrium for this algorithm.[24] The behavior of the Wolff algorithm in the critical and subcritical regions can be understood by considering the sizes of the clusters that are flipped. At low-temperatures p is near one and typical spin configurations are ordered so clusters often contain most of the sites of the system. As a result, in the subcritical region, the algorithm frequently jumps between the coexisting phases. At the critical point there is a power law distribution of cluster sizes so that the algorithm modifies the spin configuration on all length scales. In both cases, equilibration requires a number of Monte Carlo sweeps that increases as a small power of the system length. This is in contrast to the Metropolis algorithm where the equilibration time grows approximately as the square of the system length at criticality and exponentially in the system length in the coexistence region.

For Ising systems with fields such as defined in Eq. (4) the standard Wolff algorithm is not effective because a Boltzmann factor involving the fields is needed to decide whether to flip the clusters. Large clusters are pinned by the fields and the efficiency of the algorithm is lost. The two-replica algorithm[13–15] overcomes this difficulty by growing clusters in two independent replicas of the system. The replicas are noninteracting and each is described by the same Ising Hamiltonian, in this case Eq. (4). Each site of the underlying lattice is thus associated with a pair of spins, one spin belonging to each replica. A site where the spins in the two replicas are opposite is called an *active* site, otherwise it is called *inactive*. A cluster is grown from a randomly chosen active site in the same way as in the Wolff algorithm except that spins added to the cluster must agree with the seed spins for each replica. New sites that agree with the seed site are added with probability $p = 1 - e^{-4K/k_B T}$. Since there are two different interaction strengths in Eq. (4) the probability of adding a new site to the cluster is determined by the particular interaction, K_{ij} for the bond connecting the new site to the cluster. After a cluster of active sites is grown, it is

flipped by changing the sign of every spin in the cluster. Since the spins in the cluster are opposite in the two replicas, the cluster flip can also be viewed as exchanging magnetization between replicas. The advantage of the two-replica method is that there is no change in field energy of the overall system due to a cluster flip and thus no Boltzmann factor preventing clusters from flipping. It is still the case that the active clusters are usually large in the subcritical region and have a power law distribution of sizes at the critical point.

Cluster flips in the two-replica algorithm do not affect inactive sites and do not allow active sites to become inactive or vice versa. Thus, as it stands, the algorithm is not ergodic. In order to insure ergodicity, we also carry out Metropolis updates of each of the replicas separately. Equilibration is further accelerated by translating one replica relative to the other by a randomly chosen lattice vector of the underlying Bravais lattice. It is straightforward to show that the full algorithm including two-replica cluster flips, Metropolis sweeps and random translations is ergodic and satisfies detailed balance. A full discussion of the two-replica algorithm can be found in Refs. 13–15.

In order to study the coexistence curve and critical point it is necessary to locate the coexistence values of the chemical potential. In the Ising picture, the chemical potential appears as a term in the internal fields h_1 and h_2. The system is extremely sensitive to changes in the chemical potential, which must be adjusted to within one part in 10^5 to achieve phase coexistence. We determined the coexistence value of the chemical potential by using a feedback mechanism based on the clusters grown by the algorithm. As discussed above, in the subcritical region the active cluster is likely to be large. As will be shown in a forthcoming paper, at coexistence, the net magnetic field acting on large active clusters must vanish on average. Furthermore, away from coexistence, there are no large active clusters but the inactive clusters must have a net field on them that is positive in the $+$ phase and negative in the $-$ phase. The net field on a cluster is the sum of h_i over the sites of the cluster where h_i is the local field at site i. In our case, h_i takes one of two values, h_1 and h_2. Our feedback mechanism works as follows. For an initial period, both active and inactive clusters are grown and the net field acting on all clusters is averaged. If the average net field is positive it is an indication that the system is in the $+$ phase and the chemical potential is increased or vice versa (recall that the chemical potential appears with a negative sign in h). Adjustments are made in the chemical potential until the average net field on the clusters vanishes. In this way we can locate the coexistence value of the chemical potential. After the coexistence chemical potential is determined, the feedback mechanism is turned off, and the algorithm is run as described above, growing and flipping only the active clusters. During the equilibrium simulation each replica frequently jumps between the coexisting phases.

Finally, to determine the critical temperature, we monitored the susceptibility of the Ising system for a range of temperatures near the critical temperature. The susceptibility is efficiently estimated by the average size of the nonspanning active clusters.[24] We estimated the finite size critical temperature as the temperature that gave the maximum of the susceptibility. The errors quoted for the critical temperature are determined by the distance to nearby temperatures where the susceptibility is definitively less than the maximum.

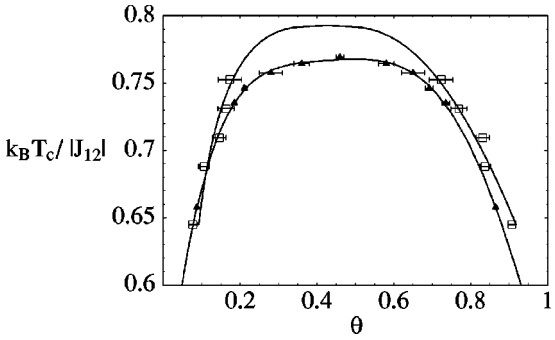

FIG. 2. Coexistence curves for $\Delta s = 1.98 k_B$, $\varepsilon_1 = -0.63$ eV, $\varepsilon_2 = -0.78$ eV, $J_{22} = J_{12} = -0.04$ eV from Ref. 6 (squares) and this work (triangles). θ is the fractional coverage.

To simulate benzene adsorption in Na–X and Na–Y zeolites we used the lattice model described in Sec. II mapped into the Ising model, Eq. (4). The centers of the zeolite cages, represented by cubes in Fig. 1, form a diamond lattice. Each unit cell of the Na–X and Na–Y framework contains eight such cages. Therefore, each unit cell of our model lattice contains 32 B sites and 16 W sites. We simulated a system with $10 \times 10 \times 10$ unit cells with periodic boundary conditions, making a total of 32 000 B and 16 000 W binding sites. We fixed the interaction parameter $J_{12} = -0.04$ eV throughout, and varied other parameters in physically relevant ranges.

Each run consisted of an initial 3000 Monte Carlo sweeps with the feedback procedure during which the coexistence chemical potential is determined and then an additional 3000 Monte Carlo sweeps to collect equilibrium data without the feedback mechanism. A single, full Monte Carlo sweep consists of one cluster sweep and one Metropolis sweep. A cluster sweep is obtained by forming as many clusters as is needed to flip (on average) each spin once. The statistical errors were calculated with the bootstrap method.[25] The simulations were performed on a 450 MHz Pentium III computer. The simulation time was 9.5×10^{-5} CPU seconds per spin per MC sweep.

IV. RESULTS

In this section we show results of MC simulations exploring how the critical point for benzene in Na–X and Na–Y changes with host–guest and guest–guest energies.

Figure 2 shows the coexistence curves obtained from this work using a $10 \times 10 \times 10$ simulation cell, as well as the result obtained from simulating a $2 \times 2 \times 2$ cell in Ref. 6. In both cases we set $\Delta s = 1.98 k_B$, $\varepsilon_1 = -0.63$ eV, $\varepsilon_2 = -0.78$ eV and $J_{22} = -0.04$ eV. For these values of the parameters we predict $T_c = 360 \pm 2$ K compared to the result from Ref. 6, $T_c = 370 \pm 8$ K. Part of this difference may arise from the different system size, while another part arises from the uncertainties in the extrapolation in Ref. 6 of the coexistence curve into the critical region. No extrapolation is

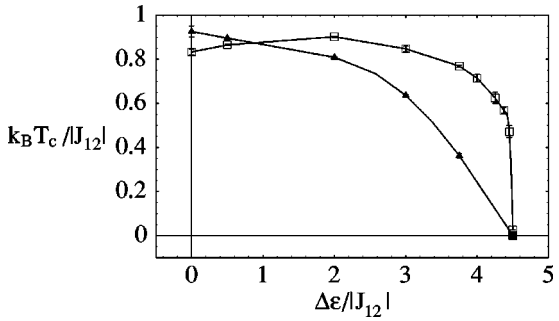

FIG. 3. T_c vs $\Delta\varepsilon \equiv \varepsilon_1 - \varepsilon_2$ for $\Delta s = 0$ (triangles) and $\Delta s = 1.98 k_B$ (squares), $J_{22} = J_{12} = -0.04$ eV.

needed in the present approach. The curve from Ref. 6 is a fit to an assumed Ising scaling law of the form $T - T_c = A(\theta - \theta_c)^3$, while the curve from the two-replica algorithm is a fifth order polynomial fit.

Figure 3 shows the critical temperature as a function of the difference in the binding energies of the W and B sites for a system with no entropy difference between the two sites (triangles) and with an entropy difference of $\Delta s = 1.98 k_B$ between the sites (squares). The data in Fig. 3 were obtained by fixing $\varepsilon_2 = -0.78$ eV, $J_{22} = J_{12} = -0.04$ eV and by varying ε_1. As the difference in the binding energies increases, the critical temperature is driven to zero. For $\Delta\varepsilon > 4.5|J_{12}|$ there is no phase coexistence. The introduction of an entropy difference between the binding sites extends the range in $\Delta\varepsilon$ for which T_c remains high, but does not change the value of $\Delta\varepsilon$ where T_c vanishes. The data for $\Delta s = 1.98 k_B$ implies that a slight change of the binding energies in the region near $\Delta\varepsilon/|J_{12}| = 4.5$ determines whether or not there is a phase transition near room temperature. Figure 3 shows that for our best estimate of $\varepsilon_1 = -0.63$ eV, removing the entropy difference between sites reduces T_c by 53%, from 360 to 170 K.

The points on the abscissas ($T_c = 0$) in Figs. 3 and 4 were obtained from a theoretical calculation of the ground-state energies of the equivalent Ising model. The ground states are expected to be ordered in one of two ways. If the magnitude of the field difference $|h_2 - h_1|$ is less than a critical value, there are two ground states, one with all spins $+1$ and the other with all spins -1. The energy per spin $E_\pm$ for these states is, respectively,

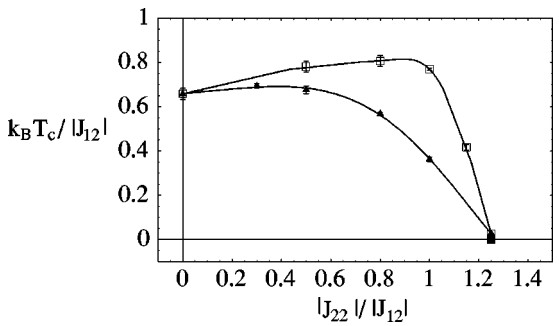

FIG. 4. T_c vs J_{22} for $\Delta s = 0$ (triangles) and $\Delta s = 1.98 k_B$ (squares), $J_{12} = -0.04$ eV, $\varepsilon_1 = -0.63$ eV, $\varepsilon_2 = -0.78$ eV.

$$E_\pm = 12K_{12} + 6K_{22} \pm 2h_1 \pm 4h_2. \tag{5}$$

On the other hand, if the magnitude of the field difference is greater than the critical value, the ground state has each spin aligned with its local field. The energy of this state is

$$E_3 = -12K_{12} + 6K_{22} - 2h_1 + 4h_2. \tag{6}$$

If the magnitude of the field difference has its critical value, the two ordered phases have the same energy. Setting the energies of staggered and magnetized states equal, we obtain

$$h_1 = h_2 - 9K_{12}. \tag{7}$$

This yields the following relation for the lattice gas parameters that make T_c vanish:

$$\Delta\varepsilon_c = 3(J_{22} - J_{12}) - \tfrac{9}{2} J_{12}. \tag{8}$$

The values of the parameters at the points on the abscissas ($T_c = 0$) in Figs. 3 and 4 are obtained from Eq. (8).

The result that the critical temperature and the existence of the transition depend sensitively on the energy difference between the binding sites is not surprising in light of results from related lattice models. For example, the Ising ferromagnet on a checkerboard lattice (bipartite lattice) with a staggered field is well-known to have a transition temperature that can be driven to zero as the strength of the staggered field is increased.[25] At a critical value of the staggered field the transition is eliminated. For values of the field near and below this critical field, the transition temperature varies strongly with field. In general, for lattices with the property that long paths must visit two types of sites with different fields, the transition temperature may be driven to zero by increasing the field difference. Interpreted as a lattice gas, the Ising model in a staggered field corresponds to a system with two binding energies whose difference is related to the staggered field. Although the decorated diamond lattice employed to model benzene Na–X and Na–Y is not bipartite, it does share the property that there are two binding energies and that long paths through the lattice must visit both types of sites.

The present lattice model for benzene in Na–X and Na–Y involves two types of guest–guest interactions: J_{22} controls intracage benzene–benzene coupling while J_{12} mediates cage-to-cage interactions. Since lattice models with only one guest–guest coupling parameter exhibit $T_c \propto |J|$, it is interesting to determine how T_c varies with J_{22} in the present system. It is logical to surmise that $T_c \propto |J_{12}|$, since this coupling parameter can lead to cooperative interactions over long length scales. However, it is not obvious how T_c varies with J_{22}. To explore this dependence, we have found the critical point for various values of Δs and J_{22}, keeping J_{12} and $\Delta\varepsilon$ fixed. Figure 4 shows the dependence of the critical temperature on the interaction between B–B sites for $\Delta s = 1.98 k_B$ (squares) and for $\Delta s = 0$ (triangles). In both cases $\varepsilon_1 = -0.63$ eV, $\varepsilon_2 = -0.78$ eV and $J_{12} = -0.04$ eV. The maximum value of J_{22} above which the system does not undergo phase transition is obtained from Eq. (8).

The phase transition suppression caused by increasing $|J_{22}|$ arises because J_{22} modifies the total field on B sites. In particular, increasing the overall stability of B sites by in-

creasing $|J_{22}|$, while keeping all other parameters fixed, effectively decreases the stability of W sites. As we have seen above, there exists a critical stability of W sites below which the phase transition is completely suppressed.

V. DISCUSSION AND CONCLUSIONS

We have performed two-replica cluster Monte Carlo (MC) simulations of benzene in Na–X and Na–Y, using a lattice model with two types of binding sites. We have calculated the critical properties of these systems for a wide range of parameters, using the particularly efficient sampling afforded by the two-replica cluster algorithm. For benzene in Na–X, critical temperatures as high as 300–400 K are found for reasonable values of the parameters, while for benzene in Na–Y no phase transition is predicted. Such high values of T_c may not seem surprising when compared to that for bulk benzene, i.e., $T_c=562$ K. However, the critical temperatures calculated above are considerably larger than those typically associated with fluids confined in microporous solids.[3,4,26] The range of critical temperatures obtained from our model of benzene in Na–X remains relatively high because of strong attractions between benzene molecules in adjacent cages. These interactions are mediated by benzene molecules in W sites, which are shared between adjacent supercages, thereby stabilizing large clusters of coupled benzenes. For benzene in Na–Y, our simulations predict that the Na–Y W site is too unstable to support the development of such large clusters.

Our predicted T_c for benzene in Na–X has important experimental consequences for adsorption and diffusion of strongly associating fluids confined in micropores.[27,28] In particular, cluster formation in subcritical systems may suggest a diffusion mechanism involving ''evaporation'' of molecules from clusters that span several cages. Such a transport mechanism is expected to give a self-diffusion coefficient with a relatively weak loading dependence,[27] which is precisely what is observed for water and ammonia diffusion in Na–X.[29]

Despite these insights, it remains troubling that the predicted vapor–liquid phase transition has not yet been observed experimentally for benzene in Na–X. Although hysteresis has been observed in adsorption isotherms measured for benzene in Na–X,[30] this observation must arise from a structural transformation of the zeolite rather than from cooperative interactions among guests, because the measured densities in the adsorption branch *exceed* those in the desorption branch. While it is possible that more careful measurements of adsorption heats and isotherms for benzene in Na–X will reveal a vapor–liquid phase transition, it is also possible that the critical temperature of benzene in Na–X is not as high as we predict. It is even possible that the energetic heterogeneity experienced by benzene in Na–X eliminates phase coexistence altogether. Indeed, our calculations predict that the critical temperature of benzene in Na–X vanishes precipitously with increasing energy difference between B and W sites, especially when W sites are favored entropically. In particular, when $(\varepsilon_1-\varepsilon_2)/|J_{12}|$ exceeds 4.5, the critical temperature vanishes along with the phase transition.

This sensitivity underscores the importance of obtaining more precise structural information for benzene in the Na–X W site, to quantify its energy and entropy more accurately. In particular, we need to know the extent to which benzene binds onto Na cations in the plane of the 12-ring window [so-called Na(III′) cations], as well as the extent to which benzene binds onto Na cations off the 12-ring window in the so-called Na(III) position. Because these benzene binding sites lack much of the symmetry of the Na–X framework, these sites are difficult to discriminate by powder neutron diffracton.[17] Single crystal neutron diffraction studies of benzene in Na–X would provide more structural information, but these measurements require relatively large Na–X crystals.[18]

In addition, we need to know the distribution of Na(III) and Na(III′) cations in Na–X. If these cations exhibit quenched disorder, then windows rich in these cations may present particularly deep traps for benzene, while cation-poor windows would be relatively unstable for cluster formation. Such energetic disorder would suppress T_c below that obtained from the corresponding ordered structure assumed in our simulations above. On the other hand, if these cations exhibit annealed disorder on the equilibration time scale for benzene adsorption, then our lattice model may become invalid altogether.

The disorder issue may be addressed by considering benzene in Na–LSX (Si:Al=1.0), which involves a strictly alternating pattern of Si and Al, and involves two Na cations per 12-ring window, assuming full occupation in other cation sites, namely sites I′ and II.[17,18] The energetic heterogeneity can be decreased further by considering benzene in Si–Y, the completely cation-free analogue of Na–X,[31] where zeolite–benzene interactions are weaker than they are in Na–X. As such, careful low-temperature measurements of adsorption heats and isotherms for benzene in Si–Y[21] may indeed reveal the vapor–liquid phase transition considered above.

Important computational work for the future involves performing off-lattice GCMC simulations on benzene in Na–X and in Si–Y. These calculations will likely require configurational-bias Monte Carlo[32,33] to facilitate inserting anisotropic adsorbates at high density. It is also important to simulate models of benzene in Na–X with quenched disorder in the binding energies. The associated Ising model is of the random field type and is much more difficult to simulate.

ACKNOWLEDGMENTS

This work was supported by NSF Grant Nos. DMR 9978233, CHE 9619019, and CTS 9734153. S.M.A. gratefully acknowledges support from a Sloan Foundation Research Fellowship (BR-3844) and a Camille Dreyfus Teacher–Scholar Award (TC-99-041).

[1] S. J. Gregg and K. S. W. Sing, *Adsorption, Surface Area and Porosity* (Academic, New York, 1982).
[2] *Physcial Adsorption: Experiment, Theory and Applications*, edited by J. Fraissard and W. C. Conner (NATO ASI series, Kluwer Academic, Dordrecht, 1996).
[3] R. Radhakrishnan and K. E. Gubbins, Phys. Rev. Lett. **79**, 2847 (1997).
[4] T. Maris, T. J. H. Vlugt, and B. Smit, J. Phys. Chem. B **102**, 7183 (1998).

[5] J. G. Pearson, B. F. Chmelka, D. N. Shykind, and A. Pines, J. Phys. Chem. **96**, 8517 (1992).
[6] C. Saravanan and S. M. Auerbach, J. Chem. Phys. **107**, 8120 (1997).
[7] M. F.Allen and D. J. Tildesley, *Computer Simulation of Liquids* (Oxford Science, Oxford, 1987).
[8] C. Saravanan, Ph.D. thesis, University of Massachusetts at Amherst, 1999.
[9] B. K. Peterson and K. E. Gubbins, Mol. Phys. **62**, 215 (1987).
[10] K. S. Page and P. Monson, Phys. Rev. E **54**, 6557 (1996).
[11] D. Barthomeuf and B. H. Ha, J. Chem. Soc., Faraday Trans. **69**, 2147 (1973).
[12] D. Barthomeuf and B. H. Ha, J. Chem. Soc., Faraday Trans. **69**, 2158 (1973).
[13] O. Redner, J. Machta, and L. F. Chayes, Phys. Rev. E **58**, 2749 (1998).
[14] L. F. Chayes, J. Machta, and O. Redner, J. Stat. Phys. **93**, 17 (1998).
[15] J. Machta, Int. J. Mod. Phys. C **10**, 1427 (1999).
[16] A. N. Fitch, H. Jobic, and A. Renouprez, J. Phys. Chem. **90**, 1311 (1986).
[17] G. Vitale, C. F. Mellot, L. M. Bull, and A. K. Cheetham, J. Phys. Chem. B **101**, 4559 (1997).
[18] D. H. Olson, Zeolites **15**, 439 (1995).
[19] C. Saravanan, F. Jousse, and S. M. Auerbach, Phys. Rev. Lett. **80**, 5754 (1998).
[20] F. Jousse and S. M. Auerbach, J. Chem. Phys. **107**, 9629 (1997).
[21] N. J. Henson, A. K. Cheetham, M. Stockenhuber, and J. A. Lercher, J. Chem. Soc., Faraday Trans. **94**, 3759 (1998).
[22] R. H. Swendsen and J.-S. Wang, Phys. Rev. Lett. **58**, 86 (1987).
[23] U. Wolff, Phys. Rev. Lett. **62**, 361 (1989).
[24] M. E. J. Newman and G. T. Barkema, *Monte Carlo Methods in Statistical Physics* (Oxford, Oxford, 1999).
[25] D. P. Landau, Phys. Rev. B **16**, 4164 (1977).
[26] C. Martin, J. P. Coulomb, Y. Grillet, and R. Kahn, *Fundamentals of Adsorption: Proceedings of the Fifth International Conference*, edited by M. D. LeVan (Kluwer Academic, Boston, 1996), p. 587.
[27] C. Saravanan and S. M. Auerbach, J. Chem. Phys. **110**, 11000 (1999).
[28] S. M. Auerbach, Int. Rev. Phys. Chem. **19**, 155 (2000).
[29] J. Kärger and H. Pfeifer, Zeolites **7**, 90 (1987).
[30] O. H. Tezel and D. M. Ruthven, J. Colloid Interface Sci. **139**, 581 (1990).
[31] L. M. Bull, N. J. Henson, A. K. Cheetham, J. M. Newsam, and S. J. Heyes, J. Phys. Chem. **97**, 11776 (1993).
[32] D. Frenkel and B. Smit, *Understanding Molecular Simulations* (Academic, San Diego, 1996).
[33] V. Lachet, A. Boutin, B. Tavitian, and A. H. Fuchs, J. Phys. Chem. B **102**, 9224 (1998).